The EMBO Journal vol.15 no.13 pp.3448–3457, 1996

Identification of contacts between topoisomerase I and its target DNA by site-specific photocrosslinking

JoAnn Sekiguchi and Stewart Shuman[1]

Molecular Biology Program, Sloan-Kettering Institute, New York, NY 10021, USA

[1]Corresponding author

Vaccinia DNA topoisomerase, a eukaryotic type I enzyme, binds and cleaves duplex DNA at sites containing the sequence 5′-(T/C)CCTT. We report the identification of Tyr70 as the site of contact between the enzyme and the +4C base of its target site. This was accomplished by UV-crosslinking topoisomerase to bromocytosine-substituted DNA, followed by isolation and sequencing of peptide–DNA photoadducts. A model for the topoisomerase–DNA interface is proposed, based on the crystal structure of a 9 kDa N-terminal tryptic fragment. The protein domain fits into the DNA major groove such that Tyr70 is positioned close to the +4C base and Tyr72 is situated near the +3C base. Mutational analysis indicates that Tyr70 and Tyr72 contribute to site recognition during covalent catalysis. We propose, based on this and other studies of the vaccinia protein, that DNA backbone recognition and reaction chemistry are performed by a relatively well-conserved 20 kDa C-terminal portion of the vaccinia enzyme, whereas discrimination of the DNA sequence at the cleavage site is accomplished by a separate N-terminal domain, which is less conserved between viral and cellular proteins. Division of function among distinct structural modules may explain the different site specificities of the eukaryotic type I topoisomerases.

Keywords: covalent catalysis/photocrosslinking/site-specific DNA cleavage/type I topoisomerase/vaccinia virus

Introduction

Eukaryotic type I topoisomerases break and rejoin DNA strands through a covalent protein–DNA intermediate. Reaction chemistry involves nucleophilic attack by a tyrosine moiety of the enzyme on the phosphodiester backbone of duplex DNA to form a 3′ phosphotyrosyl linkage to one of the DNA strands (Champoux, 1981). Although the distribution of topoisomerase I cleavage sites in duplex DNA is non-random (Edwards *et al.*, 1982; Been *et al.*, 1984), the principles governing cleavage site choice are not well understood. The question of how topoisomerase I recognizes and cleaves its DNA target is of considerable interest, insofar as site specificity may have implications for topoisomerase action *in vivo*, and because the topoisomerase–DNA complex is the pharmacological target of the anticancer drug camptothecin (Hertzberg *et al.*, 1989). Consequently, much attention has been focused on defining the features of the protein and the DNA that contribute to the DNA binding and the chemical steps of the topoisomerase reaction.

The first structural insights into this problem came from the mapping of the active site tyrosine of the yeast and vaccinia type I topoisomerases within a conserved motif, Ser-Lys-X-X-Tyr, situated near the carboxy-terminus of all known eukaryotic type I enzymes (Eng *et al.*, 1989; Lynn *et al.*, 1989; Shuman *et al.*, 1989). This provided the first fixed point of reference regarding the interface between topoisomerase I and its DNA target. Subsequent progress has been facilitated by the identification of DNA sites that bind cellular and viral type I topoisomerases with high affinity (Bonven *et al.*, 1985; Stevnser *et al.*, 1989; Shuman and Prescott, 1990; Shuman, 1991a,b; Christiansen *et al.*, 1993).

The vaccinia virus topoisomerase has emerged as a model for studies of topoisomerase–DNA interaction because it cleaves DNA with specificity comparable with that of a restriction enzyme. The viral topoisomerase forms a covalent adduct at sites containing a conserved pentapyrimidine sequence 5′-(C/T)CCTT$^{\downarrow}$ in the scissile strand (Shuman and Prescott, 1990). The T$^{\downarrow}$ residue (designated position +1) is linked via a 3′ phosphodiester bond to Tyr274 of the 314 amino acid vaccinia protein. A Tyr274→Phe substitution at the active site abolishes covalent catalysis. Yet, the Phe274 mutant protein retains the ability to bind non-covalently to the CCCTT motif (Shuman, 1991b; Sekiguchi and Shuman, 1994b). Thus, vaccinia topoisomerase is a site-specific DNA binding protein independent of its competence in trans-esterification.

Modification interference, modification protection and analog substitution experiments demonstrate that the vaccinia topoisomerase makes contact with specific base pairs and with the sugar-phosphate backbone of DNA within its CCCTT recognition site (Shuman and Turner, 1993; Sekiguchi and Shuman, 1994a). Base-specific contacts are made in the major groove of the DNA, whereas contacts with specific phosphates, including the scissile phosphate, are made on both strands along the minor groove. The phosphate contacts are situated on the opposite face of the DNA helix from the base-specific contacts, which implies that vaccinia topoisomerase binds circumferentially to the DNA (Sekiguchi and Shuman, 1994a).

Although contacts on the DNA target site have been mapped in detail, the protein side of the topoisomerase–DNA interface is largely uncharted. The structure of vaccinia topoisomerase in the DNA-bound state has been probed by chemical modification of amino acid side chains (Hanai and Wang, 1994) and by partial proteolysis (Sekiguchi and Shuman, 1995). Both approaches to protein footprinting demonstrate that specific sites on the enzyme

that are accessible in the free state become inaccessible upon DNA binding. However, there is no evidence that these sites are in direct contact with a constituent of the DNA target site that is relevant to specific binding or catalysis.

Our goal in the present study was to identify a second point of contact between vaccinia topoisomerase and its DNA ligand (the first being Tyr274 at the scissile phosphate), specifically a site of contact with an essential nucleotide base in the CCCTT motif. This was accomplished by UV-crosslinking the topoisomerase to DNA containing a single photoactive substituent, followed by isolation and sequencing of a peptide–DNA photoadduct. We reported previously that vaccinia Topo(Phe274) could be photocrosslinked with high efficiency to a 24 bp DNA molecule substituted uniquely with 5-bromocytosine at the +4 position of the CCCTT target site (Sekiguchi and Shuman, 1994a). Covalent adduct formation between the Br-substituted DNA strand and protein upon excitation by 302 nm UV light implied that a substituent of the polypeptide was in close proximity to the bromine atom. When crosslinking was performed on an analytical scale, up to one-fifth of the input +4BrdC DNA ligand could be linked to protein after UV irradiation. DNAs substituted with 5-Br pyrimidines at other positions in the CCCTT element were crosslinked with much lower efficiency. Because control experiments established that none of the bromine substitutions affected cleavage of the Br-containing DNA by the wild-type topoisomerase, we concluded that variations in crosslinking efficiency according to the position of the Br-substituted base reflected proximity (or lack thereof) of reactive moieties in the protein to the individual pyrimidine bases. Hence, we chose to map the site of protein crosslinking to the +4BrC-substituted DNA.

We show herein that residue Tyr70 of the topoisomerase is in intimate contact with the +4C base (CCCTT) in the major groove of the DNA helix. We propose a structural model for the topoisomerase–CCCTT interface based on available crystallographic data for a protein fragment that includes Tyr70 (Sharma *et al.*, 1994) and present mutational results that are consistent with the model. Our findings suggest how compartmentalization of function within distinct structural modules might account for the different site specificities of the eukaryotic type I topoisomerases.

Results

Identification of the site of photocrosslinking of topoisomerase to DNA

Having established that vaccinia topoisomerase can be crosslinked by UV to the +4BrC base at its target site, we sought to map the +4BrC photoadduct within the protein. Crosslinking reactions were carried out on a preparative scale using purified Topo(Phe274) protein and a 24 bp DNA that was 5′ ^{32}P-labeled in the +4BrC-substituted strand. Because the vaccinia topoisomerase normally forms a covalent intermediate with the scissile strand, the UV crosslinking studies were necessarily performed using Topo(Phe274), which is unable to transesterify but retains the ability to bind non-covalently at the CCCTT element (Shuman, 1991b; Sekiguchi and

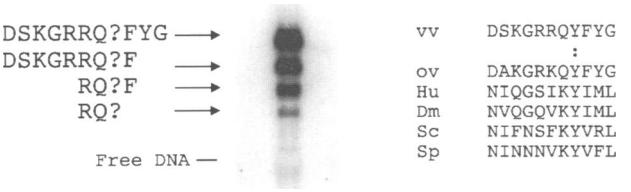

Fig. 1. Identification of the site of photocrosslinking of vaccinia topoisomerase to DNA. Topo(Phe274) was UV-crosslinked to the 5′-end-labeled 24mer DNA substrate containing a +4BrC substitution as described in Materials and methods. The products of subtilisin digestion of the isolated topoisomerase–DNA adduct were resolved by denaturing PAGE and transferred to a PVDF membrane. An autoradiogram of the membrane is shown. The free 24mer BrC-containing DNA strand migrated during electrophoresis at the position indicated on the left. The N-terminal sequence of each of the four peptide–DNA adducts is displayed on the left. Sequencing cycles in which no Edman product could be identified are indicated by a question mark (?). Shown at right is an alignment of the amino acid sequence of vaccinia topoisomerase from Asp63 to Gly73 with the homologous segments of the topoisomerases of Orf virus [another poxvirus related to vaccinia (ov)], human (Hu), *Drosophila melanogaster* (Dm), *Saccharomyces cerevisiae* (Sc) and *Schizosaccharomyces pombe* (Sp). Conservation of vaccinia residue Tyr70—the site of photocrosslinking to +4BrC—with corresponding residues in other topoisomerases is denoted by a colon (:).

Shuman, 1994b). The protein–[^{32}P]DNA photoproduct was separated from free protein by DEAE–cellulose column chromatography. Free topoisomerase flowed through the column, whereas the topo–DNA adduct bound and was eluted with 0.25 M NaCl. The [^{32}P]DNA that was not crosslinked to protein remained bound to DEAE–cellulose and could be recovered by elution with 1 M NaCl. The protein–DNA complex was subjected to proteolysis with subtilisin. Digestion products were resolved by electrophoresis through a 17% polyacrylamide gel containing 7 M urea. The peptide–DNA adducts were transferred electrophoretically to a PVDF membrane and localized by autoradiography. Four peptide–DNA adducts were resolved (Figure 1). These four species migrated more slowly during electrophoresis than the free ^{32}P-labeled 24mer DNA strand, consistent with the presence of a covalently bound peptide on the DNA. All four adducts were subjected to automated Edman sequencing. Every one of the DNA-linked peptides derived from the same region of the protein. The slowest migrating band contained the longest crosslinked peptide, extending from Asp63 to Gly73. The amino acid to which the DNA was crosslinked was inferred from the presence of an unidentifiable Edman product in the midst of an otherwise clear peptide sequence derived from the photoadduct. By this criterion, we identified Tyr70 as the site of crosslinking between Topo(Phe274) and the +4BrC base.

A structural model of the protein–DNA interface

Tyr70 is situated within a trypsin-resistant structural domain of the vaccinia topoisomerase that extends from the N-terminus to Arg80 (Sharma *et al.*, 1994; Sekiguchi and Shuman, 1995). The N-terminal domain is essential for catalysis, insofar as deletion of the first 74 amino acids of the vaccinia enzyme completely abrogates DNA relaxation and strand cleavage activities (Morham and Shuman, 1992). The structure of the isolated N-terminal

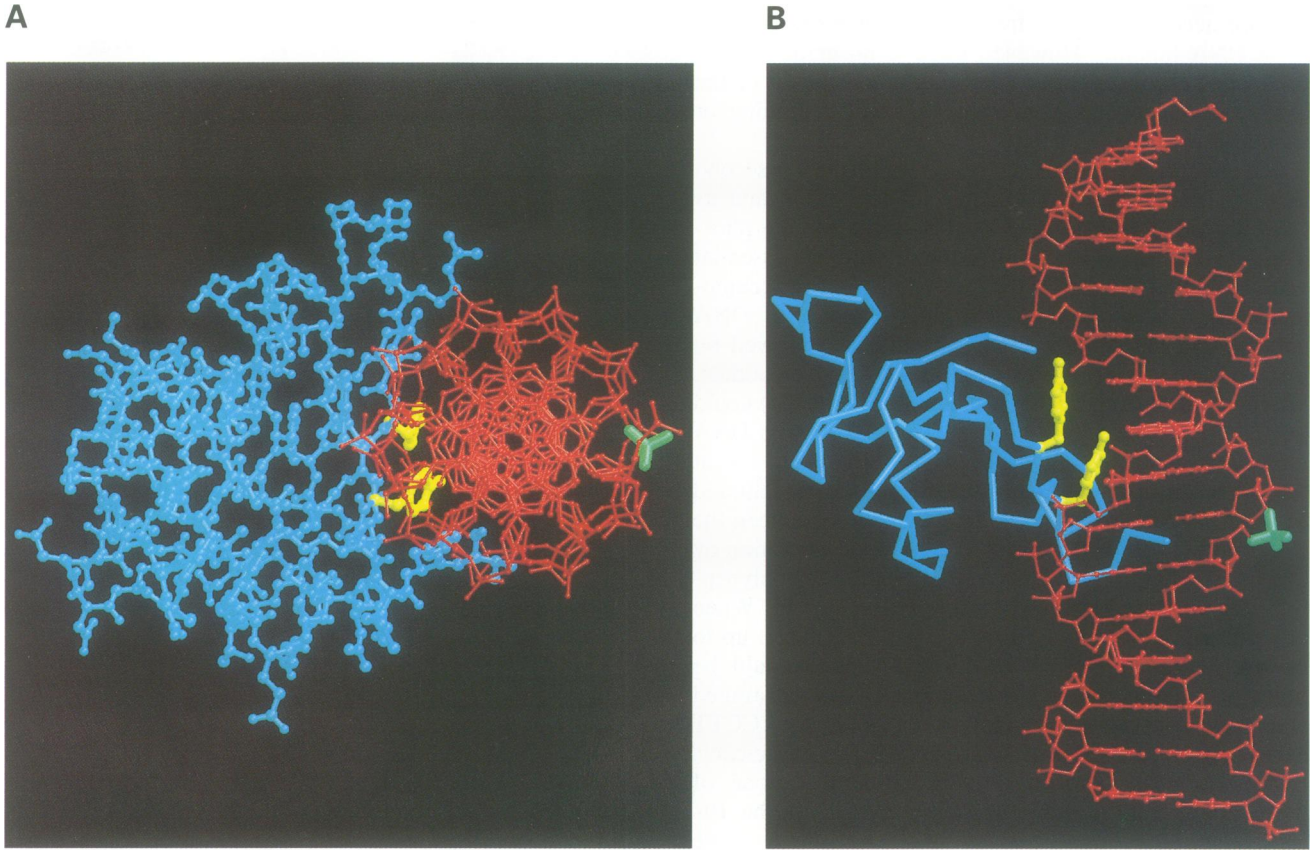

Fig. 2. Structural model of the N-terminal domain of vaccinia topoisomerase bound to the DNA target site. The published crystal structure of the N-terminal topoisomerase domain from residues 1 to 77 (Sharma *et al.*, 1994) was docked manually on a B-form CCCTT-containing DNA molecule in such a way as to place Tyr70 of the topoisomerase in proximity to C-5 of the +4 cytosine base. (**A**) A view down the DNA axis; (**B**) a longitudinal view. The images were prepared using the programs MOLSCRIPT and RASTER3D. See text for details.

domain (residues 1–77) has been determined at high resolution by X-ray crystallography (Sharma *et al.*, 1994). Our crosslinking results now suggest that this domain is involved in target site recognition. We built a molecular model of the N-terminal domain bound at the CCCTT site using the published crystal structure. The protein fitted readily into the major groove of a CCCTT-containing B-form DNA helix such that the side chain of Tyr70 was in proximity to the C-5 atom of the +4 cytosine base (Figure 2). When viewed along the helical axis, we see that the DNA (colored red) docks into a concave surface of the protein (shown as a ball-and-stick structure colored in blue). This surface is formed by a β-strand running from Arg67 to Gly73 and continuing after a sharp turn from Lys74 to Val77. The aromatic side chains of residues Tyr70 and Tyr72, which are solvent exposed in the crystal structure (Sharma *et al.*, 1994), project into the major groove of the DNA. Tyr70 and Tyr72 are highlighted in yellow in Figure 2. Tyr72 is positioned in proximity to the +3C base of the CCCTT motif. Note that the scissile phosphate, highlighted in green on the DNA, is situated on the opposite face of the helix and makes no contact with the N-terminal domain.

A longitudinal view of the model is shown in Figure 2B, with the protein backbone depicted in blue and only the Tyr70 and Tyr72 side chains highlighted in yellow. This view illustrates the proximity of the Tyr70 side chain to the +4C base and that of Tyr72 to the +3C base in the major groove. The N-terminal domain spans a region on one face of the DNA from nucleotide positions +5 to −1 (Figure 2B). It can be appreciated that the path of the protein at the C-terminus of the domain is heading toward the opposite face of the helix—the backbone trace is proceeding behind the DNA helix in the longitudinal view in Figure 2B and along the bottom of the DNA circumference in the view in Figure 2A. Greater consideration will be given to this model in the Discussion.

The principal experimental finding in support of the structural model is that Tyr70 of Topo(Phe274) crosslinks specifically to +4BrC-substituted DNA. A key prediction is that elimination of the Tyr side chain at position 70 should affect formation of the photoadduct. We tested this by mutating Tyr70 to Ala in the context of the Topo(Phe274) protein; the Y70A-Y274F double mutant protein was expressed in bacteria and purified by phosphocellulose chromatography. The extent of purification of the Y70A-Y274F protein was comparable with that of Topo(Phe274), as judged by SDS–PAGE (data not shown). Crosslinking of these two proteins to 5′ ^{32}P-labeled +4BrC-substituted 24 bp DNA was performed on an analytical scale at a 5:1 molar ratio of topoisomerase to DNA. The formation of a protein–DNA adduct between the +4BrC DNA and Topo(Phe274) was absolutely dependent on 302 nm UV irradiation, and the yield of the photoproduct increased with the duration of UV exposure (Figure 3). About 15% of the input DNA was crosslinked to Topo(Phe274) in 20 min. In contrast, the extent of crosslinking of +4BrC-DNA to the Y70A-Y274F protein (0.7% in 20 min) was

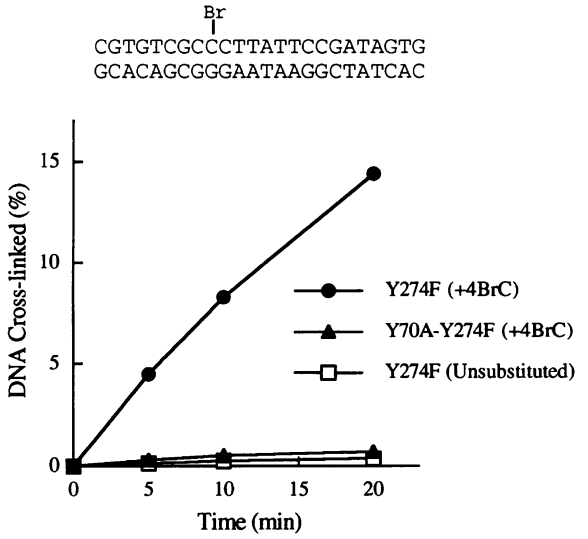

Fig. 3. Tyr70 is required for UV-crosslinking of topoisomerase to +4BrC-substituted DNA. Reaction mixtures (20 μl) containing 50 mM Tris–HCl, pH 8.0, 1 pmol of 24mer DNA duplex (5′ ^{32}P-labeled on the CCCTT-containing strand) and 185 ng of either Y274F or Y70A-Y274F proteins were incubated at 37°C for 5 min. The samples were then spotted onto parafilm and UV irradiated at 22°C for 5, 10 or 20 min. The samples were denatured immediately thereafter with 1% SDS and electrophoresed through a 10% polyacrylamide gel containing 0.1% SDS. The extent of DNA crosslinking (percent of input DNA transferred to protein) was quantitated by scanning the dried gel using a phosphorimager and was plotted as a function of the time of UV irradiation. The structure of the 24 bp DNA ligand is shown above the graph, with the site of Br substitution as indicated. A control crosslinking reaction was performed using unsubstituted 24 bp DNA.

barely above the background seen with unsubstituted DNA (0.4% in 20 min) (Figure 3). Thus, the Tyr70 side chain was required for photocrosslinking of vaccinia topoisomerase to the +4C base. Additional studies of the binding of the Topo(Phe274) and the Y70A-Y274F proteins to the 24mer DNA are presented below.

The model places Tyr72 in the major groove in the vicinity of the +3C base. Because the efficiency of crosslinking of Topo(Phe274) to +3BrC-substituted 24mer DNA was significantly lower than that of +4BrC-substituted ligand (Sekiguchi and Shuman, 1994a), we experienced difficulty mapping the site of photoadduct formation to +3BrC, i.e. the yield of peptide–DNA adduct after subtilisin digestion and transfer to PVDF was often too low to obtain the sequence beyond a few residues. However, the sequences we did obtain placed the crosslink within the N-terminal topoisomerase domain, at a site downstream of Asp63 (i.e. two different peptide–DNA adducts had N-termini at Asp63). Another peptide–DNA adduct yielded the sequence Tyr–Phe–(?). This is consistent with crosslinking of the +3C base to residue Tyr72; there are no other Tyr–Phe dipeptides in the topoisomerase protein.

Functional relevance of Tyr70 and Tyr72

We introduced single alanine substitutions for residues Tyr70 and Tyr72; we also made a double mutation in which both aromatic groups were replaced by alanine. The mutated proteins were expressed in bacteria and purified by phosphocellulose chromatography. In each case, the 33 kDa topoisomerase constituted the major species in the protein preparation, as determined by SDS–PAGE, and the extent of purification was essentially equivalent (Figure 4A). The purified proteins were tested for their ability to relax supercoiled plasmid DNA. The assays were performed in 0.1 M NaCl and 5 mM $MgCl_2$ under conditions of DNA excess. Specific activity was gauged by titration of equivalent amounts of each protein in 3-fold increments, proceeding from left to right within each titration series (Figure 4B, top panel). Replacement of both tyrosines by alanine caused a profound loss of catalytic activity, to <0.5% the level of the wild-type topoisomerase. The single Ala substitution at Tyr72 reduced specific relaxation activity to ~3% of the wild-type enzyme, whereas the Tyr70→Ala mutation reduced specific activity to between one-third and one-ninth of the wild-type (Figure 4B, top panel).

The profound effect of the Y72A mutation on topoisomerase activity was reflected in the kinetics of DNA relaxation (Figure 4B, bottom panel). The supercoiled plasmid DNA substrate (0.3 μg) was relaxed to completion within 15 s by 8.1 ng of wild-type topoisomerase. In contrast, in reactions containing the equivalent concentration of the Y72A protein, relaxed DNA accumulated slowly and steadily over 30 min. Hence the rate of relaxation was reduced at least two orders of magnitude by the Y72A mutation. The same amount of Y70A protein relaxed most of the substrate within 1 min, and all of the substrate within 2 min, i.e. at a rate estimated at between one-fourth and one-eighth that of the wild-type topoisomerase. The same amount of the Y70A-Y72A double mutant catalyzed essentially no DNA relaxation during a 30 min incubation (not shown).

Mutational effects on transesterification

An 18 bp 'suicide' substrate containing a single CCCTT cleavage site was used to examine DNA cleavage under single-turnover conditions (Figure 5). Covalent complex formation by topoisomerase on the 18mer substrate is accompanied by spontaneous dissociation of the 3′ portion of the cleaved strand (a 6 nt leaving group). With no readily available acceptor for religation, the topoisomerase becomes covalently trapped on the DNA. Cleavage was assayed by transfer of the 5′ ^{32}P-labeled scissile strand to the topoisomerase to form an SDS-resistant protein–DNA complex that was resolved from free DNA by SDS–PAGE. The extent of cleavage by wild-type topoisomerase during a 2 min reaction was proportional to added enzyme; >80% of the labeled substrate became covalently bound at saturation (Figure 5, left panel). The Y70A-Y72A double mutant was virtually inert in strand cleavage. The Y72A protein cleaved the 18mer to ~5% the level of the wild-type topoisomerase, whereas the Y70A protein formed ~60% as much covalent adduct as the wild-type enzyme in the linear range of the titration curve (Figure 5, left panel).

Suicide cleavage by the wild-type enzyme was virtually complete within 10–15 s at 37°C (Figure 5, right panel, and other data not shown). Thus, measurements of covalent adduct formation after a 2 min reaction may underestimate mutational effects on reaction rate. We therefore measured the rate of DNA cleavage by equivalent concentrations of wild-type and mutant topoisomerases (Figure 5). Although cleavage by the wild-type topoisomerase was too fast to

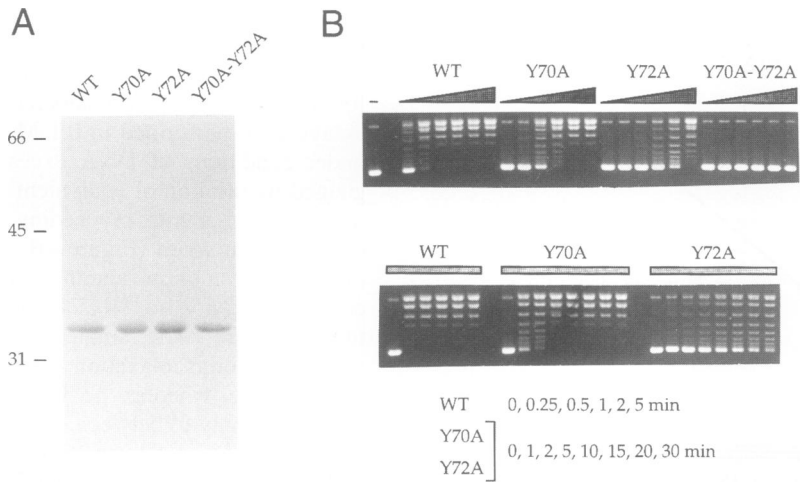

Fig. 4. Alanine substitutions for Tyr70 and Tyr72 affect topoisomerase activity. (**A**) Protein purification. Aliquots (5 μg) of the phosphocellulose preparations of wild-type topoisomerase (WT) and the Y70A, Y72A and Y70A-Y72A mutant proteins were analyzed by electrophoresis through 10% polyacrylamide gels containing 0.1% SDS. Polypeptides were visualized by staining with Coomassie blue dye. The positions and sizes (in kDa) of co-electrophoresed marker proteins are indicated on the left. (**B**) Top panel: enzyme titration. Reaction mixtures (20 μl) containing 50 mM Tris–HCl, pH 8.0, 0.1 M NaCl, 5 mM $MgCl_2$, 0.3 μg of supercoiled pUC19 DNA and (proceeding from left to right within each titration series) either 0.1, 0.3, 0.9, 2.7, 8.1 or 24.3 ng of the WT, Y70A, Y72A or Y70A-Y72A proteins were incubated at 37°C for 15 min. A control reaction (lane –) contained no topoisomerase. The reactions were halted by addition of a stop solution containing glycerol, xylene cyanol, bromophenol blue, SDS (0.2% final concentration) and EDTA (20 mM final concentration). The samples were analyzed by electrophoresis through a 1% agarose horizontal slab gel in Tris–glycine buffer (50 mM Tris, 160 mM glycine). After staining for 15 min in 0.5 μg/ml ethidium bromide solution, the gels were destained in distilled water for 30 min and then photographed under short wave UV illumination using Polaroid Type 57 film. Bottom panel: kinetics. Reaction mixtures contained (per 20 μl) 50 mM Tris–HCl, pH 8.0, 0.1 M NaCl, 5 mM $MgCl_2$, 0.3 μg pUC19 DNA and 8.1 ng of the wild-type, Y70A or Y72A protein preparation. The reactions were initiated by the addition of enzyme. Aliquots (20 μl) were withdrawn at the times indicated and quenched immediately by addition of stop solution. Samples were analyzed by agarose gel electrophoresis. The time course of relaxation is displayed from left to right within each reaction series. Incubation times are indicated below the ethidium-stained gel.

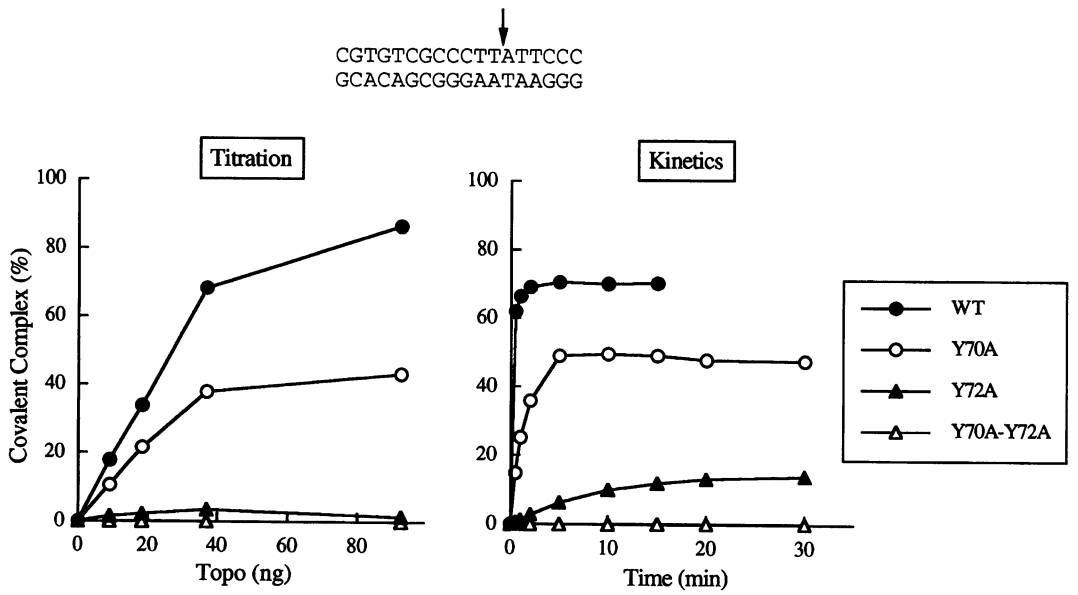

Fig. 5. Alanine substitutions for Tyr70 and Tyr72 affect DNA cleavage. The structure of the 18 bp DNA substrate is shown with the site of strand cleavage indicated by the arrow. The DNA duplex was uniquely 5′ ^{32}P-labeled on the CCCTT-containing strand. Left panel: protein titration. Reaction mixtures (20 μl) containing 50 mM Tris–HCl, pH 8.0, 5 mM $MgCl_2$, 0.5 pmol of 18 bp DNA and topoisomerase as indicated were incubated at 37°C for 2 min. The reactions were halted by addition of SDS to 1% and the samples were then electrophoresed through a 10% polyacrylamide gels containing 0.1% SDS. Strand cleavage was evinced by transfer of the radiolabeled DNA to the topoisomerase polypeptide and was quantitated by scanning the dried gel using a FUJIX BAS1000 phosphorimager. The extent of cleavage (% of labeled DNA transferred to protein) is plotted as a function of the amount (ng) of topoisomerase added. Right panel: time course. Reaction mixtures contained (per 20 μl) 50 mM Tris–HCl, pH 8.0, 5 mM $MgCl_2$, 0.5 pmol of 5′ ^{32}P-labeled 18mer and 60 ng of either wild-type topoisomerase or Y70A, Y72A or Y70A-Y72A mutant enzymes. The reactions were initiated by the addition of enzyme. Aliquots (20 μl) were removed at the indicated times and immediately denatured by addition of SDS. The samples were analyzed by electrophoresis through 10% SDS–polyacrylamide gels. The extent of strand cleavage is plotted as a function of incubation time.

determine an initial rate without using a rapid mixing–quenching apparatus (Stivers *et al.*, 1994a), we were able to measure initial rates for the Y70A and Y72A mutants. The rate of cleavage by Y70A was reduced by at least a factor of 5 relative to the wild-type. The rate of cleavage by Y72A was reduced to <1% of the wild-type value. Covalent adduct formation by an equivalent amount of the Y70A-Y72A double mutant was negligible during incubation for up to 30 min (Figure 5, right panel). The magnitude of the mutational effects on cleavage rate was entirely consistent with the effects of the individual and double alanine substitutions on DNA relaxation.

Tyr70 is important for cleavage at a subset of topoisomerase target sites

Topoisomerase action on a complex DNA molecule like pUC19 is not restricted to a single site as it is in the suicide cleavage substrate. Rather, the wild-type enzyme can bind and cleave at multiple sites on the plasmid DNA; such sites, when mapped at nucleotide resolution, contain the pentameric motif 5′-(C/T)CCTT immediately preceding the site of strand scission (Shuman and Prescott, 1990). Given that Tyr70 interacts directly with a specific nucleotide base in the CCCTT recognition element, we considered the possibility that elimination of the aromatic side chain might alter the site specificity of the topoisomerase. This was tested by incubating wild-type and Y70A topoisomerases with linear pUC19 DNA that had been cut with *Xba*I and 3′ end-labeled with [α-^{32}P]dCMP on both DNA strands. Addition of SDS to the mixture traps the covalently bound protein on the unlabeled portion of the DNA strand, permitting localization of the sites of strand cleavage by size analysis of the cleavage products under denaturing conditions. The sizes of the radiolabeled cleavage products reflect the distance of the cleavage sites from the 3′ end of the cleaved strand. As reported previously (Shuman and Prescott, 1990), the wild-type enzyme cleaved at two 'high affinity' sites at low enzyme concentration (1 ng of protein in Figure 6A). The 3′-labeled cleavage products migrated at ~2.0 and 1.6 kb during denaturing PAGE (denoted by arrows in Figure 6). Addition of more enzyme resulted in occupancy of multiple additional sites, seen as the appearance of new cleavage products of distinct size at 5 and 25 ng of input protein (Figure 6A). (The new cleavages occur at sites interposed between the high affinity sites and the 3′ ^{32}P-labeled DNA ends; as a result, the intensity of the labeled 2.0 and 1.6 kb cleavage products may decrease at high enzyme concentrations when more than one topoisomerase molecule is bound per DNA.)

Individual cleavage sites could be assigned to either the upper or lower strands of pUC19 by performing the cleavage reaction with uniquely end-labeled fragments of pUC19 DNA that were generated by digestion of the 3′-labeled *Xba*I fragment with either *Eco*RI or *Hin*dIII (Figure 6). At the level of resolution afforded by polyacrylamide gel electrophoresis, we detected eight cleavage sites on the lower strand and seven cleavage sites on the upper strand of pUC19 in the presence of 25 ng of wild-type topoisomerase (Figure 6B, WT lanes L and U). Higher levels of wild-type enzyme did not yield any additional cleavage products (not shown).

Cleavage of pUC19 by the Y70A protein was limited

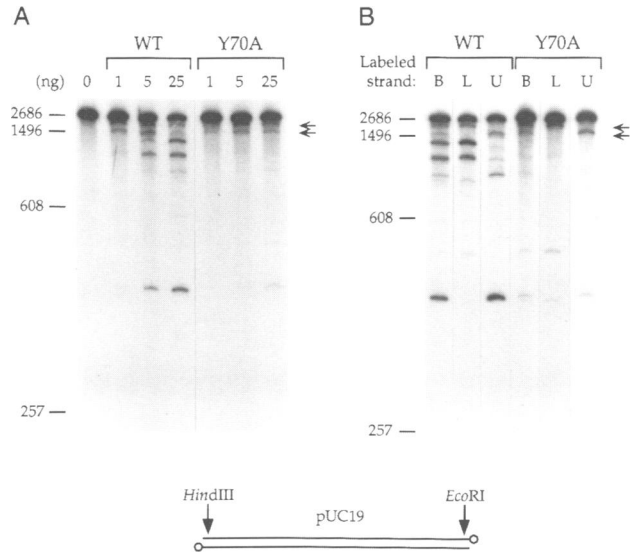

Fig. 6. The Y70A mutation affects cleavage site choice. pUC19 DNA was linearized with *Xba*I and 3′ end-labeled on both strands with [α-^{32}P]dCMP using Klenow DNA polymerase. DNAs end-labeled uniquely on either the top or bottom strands of pUC19 were prepared by secondary cleavage of the [α-^{32}P]dCMP-labeled *Xba*I fragment at nearby *Hin*dIII or *Eco*RI restriction sites. The upper and lower strands are designated according to the diagram shown at the bottom of the figure; the 3′ ends are denoted by open circles. (**A**) Reaction mixtures (20 μl) containing 50 mM Tris–HCl, pH 8.0, 10 ng of 3′-end-labeled *Xba*I-cut pUC19 DNA and either 1, 5 or 25 ng of wild-type (WT) or Y70A topoisomerase were incubated at 37°C for 10 min. Reactions were halted by addition of SDS (0.2% final concentration). The samples were adjusted to 50% formamide then heated at 95°C for 5 min. Cleavage products were analyzed by electrophoresis through a 4% polyacrylamide gel containing 7 M urea in TBE. An autoradiograph of the gel is shown. A control reaction (lane 0) contained no topoisomerase. The positions and sizes (nt) of denatured end-labeled DNA markers are indicated on the left. The products of cleavage at so-called high affinity sites are denoted by arrows at right. (**B**) Reaction mixtures (20 μl) containing 50 mM Tris–HCl, pH 8.0, 10 ng of pUC19 DNA 3′ end-labeled either on both strands (lanes B), the lower strand (lanes L) or the upper strand (lanes U), and 25 ng of either wild-type (WT) or Y70A topoisomerase were incubated at 37°C for 10 min. Cleavage products were analyzed as described above. The positions and sizes of marker DNA fragments are indicated on the left.

to a small subset of the sites that were cleaved by the wild-type topoisomerase (Figure 6A). The two sites that were cleaved best by Y70A were the two sites that were occupied by the wild-type enzyme at low protein concentration (yielding a 2 kb fragment from the lower strand and a 1.6 kb product from the upper strand) (Figure 6B). Cleavage at these sites by Y70A required slightly more input protein than did cleavage by the wild-type enzyme (Figure 6A). Y70A cleaved pUC19 at two other sites on the lower strand that were cleaved by wild-type topoisomerase (located ~400 and 525 nt from the labeled 3′ end; Figure 6B). The Y70A mutation reduced or eliminated strand scission at most other target sites, including the two sites on the lower strand of pUC19 that were cleaved to a high extent by 25 ng of wild-type topoisomerase (Figure 6B, compare the ~1.4 and 1.2 kb cleavage products in lane L of WT versus Y70A) and a site on the upper strand situated ~430 nt from the labeled 3′ end (Figure 6B, compare lane U of WT versus Y70A). It is noteworthy that elimination of the Tyr70 side chain did not result in cleavage by Y70A at sites not normally cleaved by the wild-type enzyme.

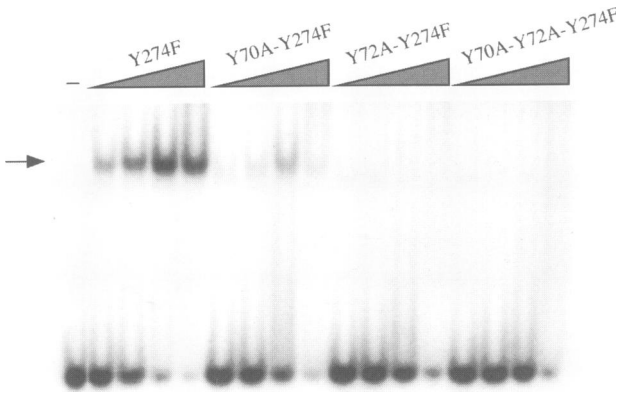

Fig. 7. Alanine substitution for Tyr70 and Tyr72 affects non-covalent DNA binding. Reaction mixtures (20 μl) containing 50 mM Tris–HCl, pH 8.0, 1 pmol of 24 bp DNA (5′ ^{32}P-labeled on the CCCTT-containing strand) and increasing amounts of purified topoisomerase as indicated (19, 37, 74 and 185 ng, corresponding to ~0.5, 1, 2 and 5 pmol, proceeding from left to right within each titration series) were incubated at 37°C for 5 min. A control reaction contained no topoisomerase (lane –). Glycerol was added to 5% and the samples were electrophoresed through a 6% native polyacrylamide gel in 0.25× TBE (22.5 mM Tris borate, 0.6 mM EDTA) at 100 V for 2.5 h. Free DNA and a topoisomerase–DNA complex of retarded mobility (denoted by an arrow at left) were visualized by autoradiographic exposure of the dried gel. The nucleotide sequence of the 24 bp DNA was the same as that shown in Figure 3.

Cleavage of linear pUC19 DNA by the Y72A mutant protein was very weak at any level of protein tested; this was expected given the feeble activity of Y72A in transesterification on the suicide substrate. The only pUC19 cleavage products we did observe with Y72A were derived from the two high affinity sites for the wild-type enzyme (not shown).

Mutations at Tyr70 and Tyr72 affect non-covalent DNA binding

To focus exclusively on the contributions of Tyr70 and Tyr72 to non-covalent DNA binding, we mutated these residues to Ala, singly and together, in the context of the Topo(Phe274) protein. The Y70A-Y274F, Y72A-Y274F and Y70A-Y72A-Y274F topoisomerases were expressed in bacteria and purified to near homogeneity (data not shown). Non-covalent DNA binding was assessed using a native gel mobility shift assay (Sekiguchi and Shuman, 1994b), in which the binding of Topo(Phe274) to a ^{32}P-labeled 24 bp CCCTT-containing DNA was seen as the formation of a discrete protein–DNA complex of retarded electrophoretic mobility (Figure 7). The extent of complex formation was proportional to Topo(Phe274) concentration and was near quantitative at a 2:1 molar ratio of Topo(Phe274) to DNA (Figure 7). The Y70A mutant of Topo(Phe274) formed lower amounts of this protein–DNA complex compared with equivalent concentrations of Topo(Phe274) (Figure 7). We estimated that the Y70A mutation reduced DNA binding affinity by ~4-fold (e.g. simply by comparing the amount of shifted complex formed by 2 pmol of Y70A-Y274F versus that formed by 0.5 pmol of Y274F). Note that a diffuse smear of shifted material was seen in the binding reaction containing 2 pmol of Y70A-Y274F (a 2:1 ratio of protein to DNA). At 5 pmol of Y70A-Y274F (a 5:1 ratio of protein to DNA), although most of the DNA had been shifted from the position of free ligand (Figure 7), the shifted DNA was found either as a diffuse smear higher in the gel or as material retained in the sample well (not shown in the figure), rather than as a discrete protein–DNA complex such as that seen with Y274F. The diffuse smearing of the DNA ligand seen with the Y70A-Y274 mutant protein may be caused by dissociation of the mutant protein–DNA complex during the electrophoresis.

The effects of the Y72A and Y70A-Y72A mutations on DNA binding were more severe. At 2 pmol of input Y72A or Y70A-Y72A, most of the DNA remained unshifted and discrete topoiosmerase–DNA complexes were barely detectable (Figure 7). DNA binding by these mutants at a 5:1 protein:DNA ratio resulted only in a smear and a shift of the DNA to the sample well (Figure 7 and data not shown).

Discussion

We have identified by UV crosslinking the site of contact between vaccinia virus DNA topoisomerase and the +4C base of its CCCTT target site in duplex DNA. The residue in contact with the +4C base, Tyr70, is located within a 9 kDa N-terminal domain demarcated by limited proteolysis with trypsin (Sharma *et al.*, 1994; Sekiguchi and Shuman, 1995) and shown by deletion analysis to be essential for catalytic activity (Morham and Shuman, 1992). Although the crystal structure of the isolated tryptic fragment has been solved (Sharma *et al.*, 1994), no specific function had yet been assigned to this domain. The present findings suggest that the N-terminal domain of the topoisomerase recognizes the pentapyrimidine sequence in the DNA major groove.

We built a structural model of the N-terminal domain bound at the CCCTT site. The DNA fits nicely into a solvent-exposed face of the domain such that Tyr70 is positioned close to the +4C base (to which it crosslinks) and Tyr72 is situated near the +3C base. Replacement of Tyr70 by alanine abrogated photocrosslinking of the topoisomerase to +4BrC-substituted DNA, indicating that the aromatic side chain of Tyr was essential for photoadduct formation. Preliminary experiments suggest that +3BrC-substituted DNA crosslinks to the topoisomerase at or near Tyr72. The finding that the BrC moieties crosslink to tyrosine residues is consistent with model compound studies and crosslinking analyses of other protein–nucleic acid complexes showing preferential crosslinking of 5-bromopyrimidines to electron-rich aromatic amino acids during 308 nm irradiation (Willis *et al.*, 1994).

The crosslinking results and the structural model pointed toward residues Tyr70 and Tyr72 as potential determinants of site specificity. Our mutational analysis supports this view. Simultaneous substitution of both aromatic residues by alanine abrogated topoisomerase activity, as assayed by relaxation of supercoiled DNA and by single-turnover strand cleavage. The Y72A single mutation reduced topoisomerase activity and strand cleavage by two orders of magnitude. In contrast, the Y70A mutation had a much milder effect; the Y70A protein was about one-fifth as active as the wild-type enzyme in DNA relaxation and strand cleavage. The mutational effects on the initial rates of suicide cleavage at fixed protein concentration reflect

the second-order rate constants of the respective proteins in the cleavage reaction. These effects can be caused by a decrease in the rate of non-covalent association of topoisomerase with the target site, an increase in the dissociation rate, a decrease in the rate of the chemical step of cleavage by enzyme bound at the target site (k_{c1}) or any combination thereof.

A native gel-shift assay was used to assess mutational effects on DNA binding. In order to exclude the contributions of covalent adduct formation to the binding reaction, the Y70A and Y72A mutations were introduced into Topo(Phe274). The catalytically inert Topo(Phe274) formed a discrete protein–DNA complex that was stable to gel electrophoresis. The Y72A mutation reduced the formation of this complex to barely detectable levels. The Y70A mutation reduced non-covalent binding affinity by about a factor of 4. The magnitude of the effects of the Y72A and Y70A mutations on non-covalent DNA binding was broadly consistent with their effects on topoisomerase activity and single-turnover DNA cleavage. The gel shift experiments are supportive of the structural model, which places Tyr70 and Tyr72 at the protein–DNA interface.

Detection of a discrete topoisomerase–DNA complex in the mobility shift assay requires that the protein be bound stably to the DNA ligand. The smearing of the shifted DNA seen with the Y70A-Y274 mutant protein may reflect reduced stability of the mutant protein–DNA complex, which results in its dissocation during the electrophoresis. At the Y70A-Y274F protein concentration used in the UV crosslinking experiment (5-fold excess over DNA), nearly all the DNA was shifted in the native gel assay, but the complexes were not discrete. Hence, the failure to detect UV crosslinking of Y70A-Y274 to +4BrC-containing DNA in solution (Figure 3) may have a more subtle basis than mere replacement of Tyr by a non-photoreactive substitutent. Further dissection of the structural requirements for photadduct formation, as distinct from DNA binding, will hinge on the introduction of additional amino acid substitutions for Tyr70.

The finding that the Y70A mutation altered the distribution of cleavage sites in plasmid DNA provides additional evidence that Tyr70 is involved in site recognition. Some sites appeared more dependent on Tyr70 for binding and cleavage than others. This finding reinforces earlier conclusions that the topoisomerase cleavage sites in pUC19 DNA are not equivalent despite the presence of a conserved pentapyrimidine sequence. Different cleavage sites display distinct sensitivities to salt, divalent cations and temperature as reaction variables (Shuman and Prescott, 1990). It is interesting that the two sites designated previously as high affinity for the wild-type enzyme were among the ones that were still cleaved by the Y70A mutant protein. The extent of cleavage at any given site is likely to be influenced by DNA conformation and flanking sequence effects outside the pentamer motif. Unfortunately, comparison of the nucleotide sequences flanking the cleavage sites in pUC plasmid DNA provides no useful insights [refer to Shuman and Prescott (1990) for an alignment of cleavage site sequences]. Although the rules governing cleavage site strength still remain obscure, the Y70A protein should prove very useful in delineating the relevant principles, e.g. by comparative analysis of topoisomerase action on model duplex substrates corresponding to individual high and low affinity cleavage sites.

Whereas our results indicate that Tyr70 and Tyr72 are part of the DNA binding surface of the topoisomerase, they do not reveal the physical principles involved. It is possible that Tyr70 and Tyr72 form hydrogen bonds with the DNA, either directly or through bridging water molecules. More extensive mutational analysis of residues 70 and 72, as well as other amino acids along the protein–DNA surface suggested by the structural model, ought to clarify the role of the N-terminal domain in site recognition. We recognize that the model provides only a best-guess fit of the interface of the N-terminal fragment with the binding element in the DNA major groove. It is not meant to be taken as a literal map of atomic positions and distances between DNA and protein.

The N-terminal fragment is one of three structural domains of the vaccinia topoisomerase that have been identified by proteolysis. The border of the N-terminal domain is demarcated by a trypsin-sensitive peptide bond, between Arg80 and Asn81, that bridges the N-terminal domain to a 'central' structural domain extending from Asn81 to Lys135. The trypsin-sensitive bridge at Arg80 becomes highly refractory to proteolysis when the topoisomerase is bound to DNA. Although Arg80 is not included in the crystal structure of the N-terminal domain (which extends to Val77), our model of the protein–DNA complex suggests that Arg80 might be near the DNA as the path of the protein extends around the helix to the opposite face. A lysine residue near the bridge (either Lys74 or Lys83) is protected from chemical modification when the topoisomerase is bound to DNA (Hanai and Wang, 1994). The side chain of Lys74 is oriented away from the DNA in our model of the protein–DNA complex, which suggests that Lys83 is the site protected from chemical modification in the DNA-bound state. Alternatively, the orientation of the Lys74 side chain may be different in the full-sized topoisomerase and/or in the DNA-bound state than it is in the crystal structure of the isolated N-terminal domain.

A 20 kDa C-terminal domain of the vaccinia topoisomerase is connected to the central domain via a protease-accessible 'hinge' region situated between residues Lys135 and Thr147. Within the hinge region, Lys135, Tyr136 and Glu139 become protected from trypsin, chymotrypsin and V8, respectively, when topoisomerase is bound to DNA (Sekiguchi and Shuman, 1995). Specific lysine residues in this region are shielded from chemical modification when the topoisomerase is DNA bound (Hanai and Wang, 1994). It is likely, therefore, that the hinge region contacts the DNA. Mutational analysis reveals that several amino acid residues within or near the hinge are essential for DNA cleavage. If these residues are involved directly in transesterification at the scissile bond as suggested (Wittschieben and Shuman, 1994; Stivers *et al.*, 1994b), then the hinge ought to be situated in a space near the active site Tyr274 when the enzyme is bound at the target site. Unfortunately, no high resolution structural information is yet available for any portion of the topoisomerase other than the N-terminal tryptic fragment.

An important functional point is that a 20 kDa carboxyl fragment of the topoisomerase that includes the hinge binds non-covalently to duplex DNA, but does not display

the specificity for the CCCTT target site characteristic of the full-sized protein (Sekiguchi and Shuman, 1995). Requirement for the N-terminus for site specificity is entirely consistent with the structural model in which the 9 kDa N-terminal domain is bound to the CCCTT sequence in the major groove. We suggest that the hinge and C-terminal domain (which contains the active site tyrosine) make contact with the phosphodiester backbone of the DNA across the minor groove on the opposite face of the helix. We presume that the central and C-terminal domains also interact with the DNA at points flanking the CCCTT element, because it is known that the topoisomerase footprint extends for 10–12 bp on both sides of the site of strand cleavage (Shuman, 1991b; Shuman and Turner, 1993) and because the N-terminus as we model it on the DNA is insufficient to account for the footprint.

The amino acid sequence of the vaccinia topoisomerase is homologous to the sequences of topoisomerases encoded by other poxviruses and to the nuclear type I enzymes from yeast to human (Shuman and Moss, 1987; Lynn *et al.*, 1989). According to the sequence alignment of Caron and Wang (1994), Tyr70 of the vaccinia enzyme is strictly conserved at an analogous position in every one of the eukaryotic topoisomerases (Figure 1). A few other residues in the vicinity of Tyr70 also have conserved counterparts in the cellular topoisomerases, e.g. Asp63 of the vaccinia enzyme, which is Asn in several cellular enzymes, and vaccinia Gly66, which is conserved in the human and *Drosophila* proteins, but not in the yeast enzymes. The N-terminal domain as a unit is only moderately conserved at sequence level with the cellular type I enzymes (15/80 residues). The protein segments with the greatest degree of conservation are at the hinge and within the C-terminal structural domain of the vaccinia protein. This engenders a model for site recognition and catalysis that may apply to all eukaryotic type I topoisomerases, i.e. that DNA backbone recognition and reaction chemistry are performed by a relatively well-conserved protein domain corresponding to the hinge and C-terminal regions of the vaccinia enzyme, whereas discrimination of the DNA sequence at the cleavage site is accomplished by a separate domain that is less conserved between viral and cellular proteins. Side-by-side comparison of the vaccinia and human enzymes revealed no overlap whatsoever in their sites of cleavage in 3′-end-labeled pUC19 DNA (Morham and Shuman, 1992; J.Wittschieben and S.Shuman, unpublished). Mammalian topoisomerase I exhibits a rather loose sequence preference dictated by the four bases immediately 5′ of the scissile bond (Jaxel *et al.*, 1991), i.e. on the covalently held side of the nick, as in the case of the vaccinia enzyme. The base preference of the cellular topoisomerases differs sharply from the vaccinia enzyme, except for a strong bias toward a T at the scissile bond. We envisage that the stringent specificity of the vaccinia topoisomerase for the pentapyrimidine sequence is a consequence of distinctive structural features of the N-terminal domain. The structure of the analogous segment of the cellular topoisomerase I has not been reported; it would not be surprising if it differed substantially from that of the vaccinia topoisomerase.

Materials and methods

UV crosslinking of topoisomerase to DNA

Topo(Phe274) was expressed in bacteria and purified to homogeneity as described (Morham and Shuman, 1992; Sekiguchi and Shuman, 1994b). The 24 bp +4BrC-substituted DNA was prepared by 5′-end labeling the 24mer +4BrC-containing strand [5′-CGTGTCGC(BrC)CTTATT-CCGATAGTG], followed by annealing to an unlabeled 24mer complementary strand present at 4-fold molar excess (Shuman, 1991a). Reaction mixtures (1 ml) containing 50 mM Tris–HCl, pH 8.0, 10 nmol of +4BrC-substituted 24 bp DNA (5′ ^{32}P-labeled on the CCCTT-containing strand) and 50 nmol of Topo(Phe274) were incubated at 37°C for 10 min. The mixture was transferred into one 9.6 cm^2 well of a 6-well tissue culture dish and irradiated for 10 min at 22°C using a 302 nm transilluminator (UVP Model TM-36) situated 2.2 cm above the sample. The sample was mixed with an equal volume of buffer A (50 mM Tris–HCl, pH 8.0, 1 mM EDTA, 2.5 mM dithiothreitol, 10% glycerol, 0.1% Triton X-100) containing 0.1 M NaCl and 6 M urea. This material was then applied to a 1 ml DEAE–cellulose column that had been equilibrated in buffer A containing 0.1 M NaCl/6 M urea. Topoisomerase that had not been crosslinked to DNA was recovered in the flow-through fraction, whereas the radiolabeled DNA was retained on the column. The column was washed with 10 ml of the same buffer, then with 10 ml of 0.1 M NaCl in buffer A without urea. The protein–DNA photoadduct was step-eluted with 0.25 M NaCl in buffer A. Fractions (0.25 ml) were collected into siliconized microcentrifuge tubes during the elution; those containing the peak of radiolabeled DNA were pooled (1.5 ml volume; ~160 pmol of DNA). SDS–PAGE of the eluate fractions confirmed that the 42–43 kDa topoisomerase–[^{32}P]DNA photoadduct had been recovered in the 0.25 M eluate. The majority of the non-crosslinked DNA was retained on the DEAE–column and could be eluted by 1 M NaCl. The 0.25 M NaCl eluate was digested with subtilisin (60 μg) for 16 h at 22°C. The digested sample was ethanol precipitated and the pelleted material was resuspended in 8 μl of formamide. This sample was heated to 95°C for 5 min and electrophoresed through a 12% polyacrylamide gel containing 6 M urea in TBE (90 mM Tris–borate, 2.5 mM EDTA) at 60 W for 1.5 h. The resolved peptide–DNA adducts were then transferred from the gel to a PVDF membrane (Bio-Rad) in blotting buffer (10 mM CAPS, pH 11, 10% methanol) using a Hoefer Transphor apparatus (Model TE42). The electrophoretic transfer was carried out at 500 mA for 2.5 h. The membrane was rinsed in distilled water for 30 min and then air dried. Presumptive peptide–DNA adducts were localized by autoradiography. Membrane slices containing individual labeled bands were excised. Automated N-terminal sequencing of the membrane-bound material was performed using a modified model 477A microsequencer (Applied Biosystems).

Mutational analysis

Mutations in vaccinia topoisomerase were programmed by synthetic oligonucleotides using the two-stage PCR-based overlap extension strategy. Primers were designed to substitute alanine for tyrosine at positions 70 and 72 of the protein, singly and together. The mutated genes were cloned into pET3c to generate plasmids pET-Y70A, pET-Y72A and pET-Y70A/Y72A. The presence of the desired mutations was confirmed by dideoxy sequencing. The entire insert of each topoisomerase expression plasmid was sequenced to ensure that no unwanted mutations had been introduced during the PCR and cloning operations. The plasmids were transformed into *Escherichia coli* BL21. Expression of topoisomerase was induced by infection of 50 ml bacterial cultures with bacteriophage λCE6 (Shuman *et al.*, 1988). Wild-type and mutated topoisomerases were purified from soluble lysates by phosphocellulose column chromatography (Shuman *et al.*, 1988). Protein concentrations were determined using the Bio-Rad dye reagent with bovine serum albumin as the standard.

Acknowledgements

We thank Dr Alfonso Mondragon for communicating the crystallographic coordinates of the N-terminal topoisomerase domain. We thank Dr Philip Jeffrey for his invaluable help in modeling the protein–DNA complex. This work was supported by grants GM 46330 from the National Institutes of Health and FRA-432 from the American Cancer Society.

References

Been,M.D., Burgess,R.R. and Champoux,J.J. (1984) Nucleotide sequence preference at rat liver and wheat germ type I DNA topoisomerase breakage sites in duplex SV40 DNA. *Nucleic Acids Res.*, **12**, 3097–3114.

Bonven,B.J., Gocke,E. and Westergaard,O. (1985) A high affinity topoisomerase I binding sequence is clustered at DNase I hypersensitive sites in *Tetrahymena* R-chromatin. *Cell*, **41**, 541–555.

Caron,P.R., and Wang,J.C. (1994) Alignment of primary sequences of DNA topoisomerases. *Adv. Pharmacol.*, **29B**, 271–297.

Champoux,J.J. (1981) DNA is linked to the rat liver DNA nicking-closing enzyme by a phosphodiester bond to tyrosine. *J. Biol. Chem.*, **265**, 4805–4809.

Christiansen,K., Svejstrup,A.B.D., Andersen,A.H. and Westergaard,O. (1993) Eukaryotic topoisomerase I-mediated cleavage requires bipartite DNA interaction. *J. Biol. Chem.*, **268**, 9690–9701.

Edwards,K.A., Halligan,B.D., Davis,J.L., Nivera,N.L. and Liu,L.F. (1982) Recognition sites of eukaryotic topoisomerase I: DNA nucleotide sequencing analysis of topo I cleavage sites on SV40 DNA. *Nucleic Acids Res.*, **10**, 2565–2576.

Eng,W., Pandit,S.D. and Sternglanz,R. (1989) Mapping of the active site tyrosine of eukaryotic DNA topoisomerase I. *J. Biol. Chem.*, **262**, 13373–13376.

Hanai,R. and Wang,J.C. (1994) Protein footprinting by the combined use of reversible and irreversible lysine modifications. *Proc. Natl Acad. Sci. USA*, **91**, 11904–11908.

Hertzberg,R.P., Caranfa,M.J. and Hecht,S.M. (1989) On the mechanism of topoisomerase I inhibition by camptothecin: evidence for binding to an enzyme–DNA complex. *Biochemistry*, **28**, 4629–4638.

Jaxel,C., Capranico,G., Kerrigan,D., Kohn,K.W. and Pommier,Y. (1991) Effect of local DNA sequence on topoisomerase I cleavage in the presence or absence of camptothecin. *J. Biol. Chem.*, **266**, 20418–20423.

Lynn,R.M., Bjornsti,M., Caron,P.R. and Wang,J.C. (1989) Peptide sequencing and site-directed mutagenesis identify tyrosine-727 as the active site tyrosine of *Saccharomyces cerevisiae* DNA topoisomerase I. *Proc. Natl Acad. Sci. USA*, **86**, 3559–3563.

Morham,S.G. and Shuman,S. (1992) Covalent and noncovalent DNA binding by mutants of vaccinia DNA topoisomerase I. *J. Biol. Chem.*, **267**, 15984–15992.

Sekiguchi,J. and Shuman,S. (1994a) Vaccinia topoisomerase binds circumferentially to DNA. *J. Biol. Chem.*, **269**, 31731–31734.

Sekiguchi,J. and Shuman,S. (1994b) Requirements for noncovalent binding of vaccinia topoisomerase I to duplex DNA. *Nucleic Acids Res.*, **22**, 5360–5365.

Sekiguchi,J. and Shuman,S. (1995) Proteolytic footprinting of vaccinia topoisomerase I bound to DNA. *J. Biol. Chem.*, **270**, 11636–11645.

Sharma,A., Hanai,R. and Mondragon,A. (1994) Crystal structure of the amino terminal fragment of vaccinia virus DNA topoisomerase I at 1.6 Å resolution. *Structure*, **2**, 767–777.

Shuman,S. (1991a) Site-specific DNA cleavage by vaccinia virus DNA topoisomerase I: role of nucleotide sequence and DNA secondary structure. *J. Biol. Chem.*, **266**, 1796–1803.

Shuman,S. (1991b) Site-specific interaction of vaccinia virus DNA topoisomerase I with duplex DNA: minimal DNA substrate for strand cleavage *in vitro*. *J. Biol. Chem.*, **266**, 11372–11379.

Shuman,S. and Moss,B. (1987) Identification of a vaccinia virus gene encoding a type I DNA topoisomerase. *Proc. Natl Acad. Sci. USA*, **84**, 7478–7482.

Shuman,S. and Prescott,J. (1990) Specific DNA cleavage and binding by vaccinia virus DNA topoisomerase I. *J. Biol. Chem.*, **265**, 17826–17836.

Shuman,S. and Turner,J. (1993) Site-specific interaction of vaccinia virus topoisomerase I with base and sugar moieties in duplex DNA. *J. Biol. Chem.*, **268**, 18943–18950.

Shuman,S., Golder,M. and Moss,B. (1988) Characterization of vaccinia virus DNA topoisomerase I expressed in *Escherichia coli*. *J. Biol. Chem.*, **263**, 16401–16407.

Shuman,S., Kane,E.M. and Morham,S.G. (1989) Mapping the active site tyrosine of vaccinia virus DNA topoisomerase I. *Proc. Natl Acad. Sci. USA*, **86**, 9793–9797.

Stevnser,T., Mortensen,U.H., Westergaard,O. and Bonven,B.J. (1989) Interactions between eukaryotic DNA topoisomerase I and a specific binding sequence. *J. Biol. Chem.*, **264**, 10110–10113.

Stivers,J.T., Shuman,S. and Mildvan,A.S. (1994a) Vaccinia DNA topoisomerase I: single-turnover and steady-state kinetic analysis of the DNA strand cleavage and ligation reactions. *Biochemistry*, **33**, 327–339.

Stivers,J.T., Shuman,S. and Mildvan,A.S. (1994b) Vaccinia DNA topoisomerase I: kinetic evidence for general acid–base catalysis and a conformational step. *Biochemistry*, **33**, 15449–15458.

Willis,M.C., LeCuyer,K.A., Meisenheimer,K.M., Uhlenbeck,O.C. and Koch,T.H. (1994) An RNA–protein contact determined by 5-bromouridine substitution, photocrosslinking, and sequencing. *Nucleic Acids Res.*, **22**, 4947–4952.

Wittschieben,J. and Shuman,S. (1994) Mutational analysis of vaccinia virus DNA topoisomerase defines amino acid residues essential for covalent catalysis. *J. Biol. Chem.*, **269**, 29978–29983.

Received on December 13, 1995; revised on February 15, 1996